RNA Secondary Structures: A Tractable Model of Biopolymer Folding

Ivo L. Hofacker
Institut für Theoretische Chemie der Universität Wien,
Währingerstr. 17, 1090 Wien, Austria
E-mail: ivo@tbi.univie.ac.at

RNA secondary structures provide a suitable model system for studying the thermodynamics and kinetics of biopolymer folding. In contrast to models of protein folding of comparable complexity, the ground state structure as well as most thermodynamic quantities of interest, such as partition function and density of states can be calculated by efficient algorithms in polynomial time. For small RNA molecules, up to as few hundred bases, the kinetics of folding can be studied in Monte Carlo type simulations. As an example application, we consider the effect of modified bases in tRNA molecules.

1 Introduction

Folding sequences into structures is a central problem in biopolymer research. While most models of biopolymer folding are concerned with protein folding, the same questions can be posed for RNA molecules. [1] An important advantage of RNA is that, on the level of secondary structure, the structure prediction problem can be solved with reasonable accuracy. RNA secondary structures provide a discrete, coarse grained concept of structure similar in complexity to lattice models of proteins.

The ease with which structures can be predicted was exploited in previous studies for a detailed characterization of the sequence to structure map for RNA [2,3,4] and its consequences for evolutionary adaptation. [5] However, little is known about the kinetics of structure formation for RNA and related questions of "foldability". Short sequences are generally believed to fold into their thermodynamic ground state, while kinetic trapping is expected to be an important effect for longer sequences. It has become clear that a better understanding of the dynamics of biopolymer structure formation requires a rather detailed knowledge about the structure of the underlying energy surface. In the following we'll present several tools to obtain information about the energy landscape of an RNA molecule and simulate secondary structure formation. As a first application of these tolls we'll look at the folding dynamics of a transfer RNA.

2 RNA Secondary Structure and its Prediction

A secondary structure on a sequence is a list of base pairs $[i, j]$ with $i < j$ such that for any two base pairs $[i, j]$ and $[k, l]$ with $i \leq k$ holds:

$$\begin{aligned} i = k &\iff j = l \\ k < j &\Longrightarrow i < k < l < j \end{aligned} \tag{1}$$

The first condition implies that each nucleotide can take part in at most one base pair, the second condition forbids knots and pseudo-knots and guarantees that secondary structures can be represented as planar graphs. While pseudo-knots are

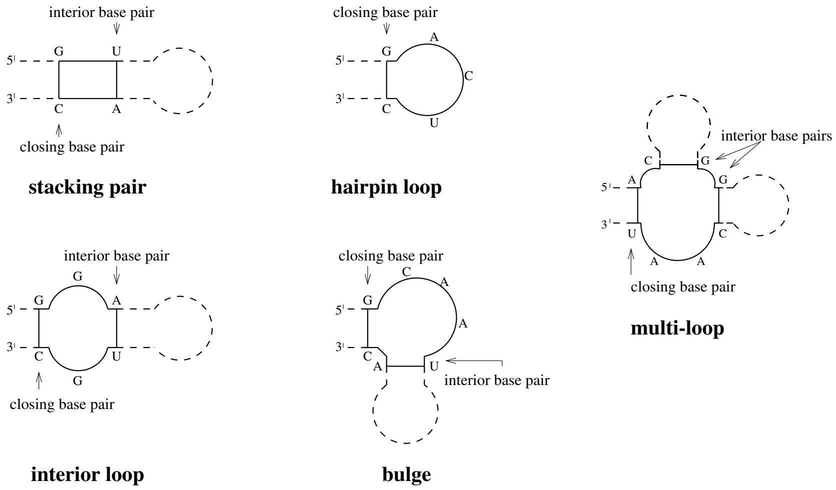

Figure 1: RNA secondary structure elements. Any secondary structure can be uniquely decomposed into these types of loops

important in some natural RNAs [6], they can be considered part of the tertiary structure for our purposes. The restriction to knot-free structures is necessary for dynamic programming algorithms. Usually, only Watson-Crick (**AU** and **GC**) and **GU** pairs are allowed.

Any secondary structures can be uniquely decomposed into loops as shown in Fig. 1 (note that a stacked base pair is considered a loop of size zero). The energy of an RNA secondary structure is assumed to be the sum of the energy contributions of all loops. Energy parameters for the contribution of individual loops have been determined experimentally (see e.g. [7,8,9]) and depend on the loop type, size and partly its sequence.

The additive form of the energy model allows for an elegant solution of the minimum energy problem through dynamic programming, that is similar to sequence alignment. This similarity was first realized and exploited by Waterman [10,11], the first dynamic programming solution was proposed by Nussinov [12,13] originally for the "maximum matching" problem of finding the structure with the maximum number of base pairs. Zuker and Stiegler [14,15] formulated the algorithm for the minimum energy problem using the now standard energy model. Since then several variations have been developed: Michael Zuker [16] devised a modified algorithm that can generate a subset of suboptimal structures within a prescribed increment of the minimum energy. The algorithm will find any structure S that is optimal in the sense that there is no other structure S' with lower energy containing all base pairs that are present in S. As noted by John McCaskill [17] the partition function over all secondary structures $Q = \sum_S \exp(-\Delta G(S)/kT)$ can be calculated by dynamic programming as well. In addition his algorithm can calculate the frequency with which each base pair occurs in the Boltzmann weighted ensemble of all possible structures, which can be conveniently represented in a "dot-plot", see Fig. 3.

The memory and CPU requirements of these algorithms scale with sequence

$$
\begin{aligned}
N^B_{ij}(\epsilon) &= \delta(\mathcal{H}(i,j),\epsilon) + \sum_{i<j<k<l} N^B_{kl}(\epsilon - \mathcal{I}(i,j,k,l)) + \\
&\quad + \sum_{i<k<j} \left[\sum_{\epsilon'} N^M_{i+1,k-1}(\epsilon')\, N^{M1}_{k,j-1}(\epsilon - \epsilon' - \mathcal{M}_C) \right] \\
N^{M1}_{ij}(\epsilon) &= \sum_{i<l\le j} N^B_{il}(\epsilon - \mathcal{M}_B(j-l) - \mathcal{M}_I) \\
N^M_{ij}(\epsilon) &= \sum_{i<k\le j} \left[\sum_{\epsilon'} N^M_{i,k-1}(\epsilon')\, N^{M1}_{kj}(\epsilon - \epsilon') \right] + \\
&\quad + \sum_{i\le k\le j} N^{M1}_{kj}(\epsilon - \mathcal{M}_B(k-i)) \\
N^A_{ij}(\epsilon) &= \sum_{i<l\le j} N^B_{il}(\epsilon) \\
N_{ij}(\epsilon) &= \delta(0,\epsilon) + N^A_{ij}(\epsilon) + + \sum_{i\le k<j} \left[\sum_{\epsilon'} N_{ik}(\epsilon') N^A_{k+1,j}(\epsilon - \epsilon') \right]
\end{aligned}
$$

Recursion for the calculation of the density of states: Calligraphic symbols denote energy parameters for different loop types: hairpin loops $\mathcal{H}(i,j)$, interior loops, bulges, and stacks $\mathcal{I}(i,j,k,l)$; the multi-loop energy is modeled by the linear ansatz $\mathcal{M} = \mathcal{M}_C + \mathcal{M}_I \cdot \text{degree} + \mathcal{M}_\text{M} \cdot \text{unpaired}$, e.g. [15] The number $N^B_{ij}(\epsilon)$ of substructures on the substring $[i,j]$ with energy ϵ subject to the condition that i and j form a base pair is determined recursively from smaller fragments. The base pair (i,j) can be the closing pair of a hairpin, it may close an interior loop (or extend a stack), or it might close a multi-loop. The auxiliary variables N^M and N^{M1} are necessary for handling the multi-loops [17], N^A helps reducing the CPU requirements. The unconstrained d.o.s. of the substring $[i,j]$ is stored in $N_{ij}(\epsilon)$. The first term accounts for the unpaired structure. The second term collects all structures that consist of a single component, possibly with an unpaired "tail" at the 3' end. The final term arises from the formal construction of multi-component structures from a 1-component part at the 3' side and an arbitrary structure at the 5' side.

length n as $\mathcal{O}(n^2)$ and $\mathcal{O}(n^3)$, respectively, making structure prediction feasible even for large RNAs of about 10000 nucleotides, such as the genomes of RNA viruses. [18,19] A freely available implementation of these algorithms is the `Vienna RNA Package`. [20,21]

McCaskill's work was extended in our group to yield an algorithm that computes the complete density of states of an RNA sequence at predefined energy resolution. [22,23] Another method for calculating a density of states, based on enumeration of structures, was proposed earlier by Higgs. [24] However, his algorithm is restricted to subset of structures containing no helices shorter than three and uses a simplified energy model. Still, our algorithm is rather demanding as it needs to store $\mathcal{O}(n^2 m)$ entries and $\mathcal{O}(n^3 m^2)$ operations to compute them, where m is the number of energy bins used. Thus it is practical only for sequences up to some 100 nucleotides. As an example for the dynamic programming ansatz an outline of the algorithm is shown in the box on the following page.

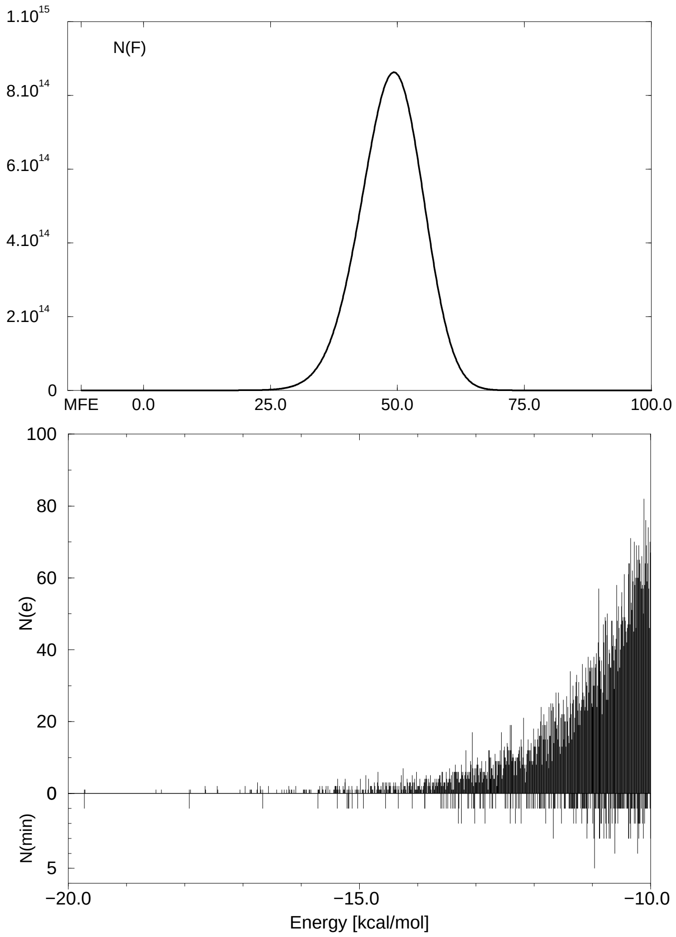

Figure 2: Density of states of the yeast $\mathrm{tRNA}^{\mathrm{phe}}$. Top: Complete Density of States computed with an energy resolution of 0.1 kcal/mol, computed using the Density of state algorithm. The total number of structures is $14,995,224,405,213,184$. Less than 2 million structures have negative energy, the reference state being the open structure. The lower figure shows the density of states and the density of local minima in the region above the native state at higher resolution. For this plot all structures within 15kcal/mol the ground state were generated by suboptimal folding and tested for being local minima. The tRNA sequence with modified bases used here displays only a few suboptimal structures within a few kT above the native state.

Finally, we have recently designed a program that can generate *all* secondary structures within some interval of the minimum energy [25], based on dynamic programming and multiple backtracking. The performance of the algorithm depends mainly on the number of structures found. Since the number of possible structures grows exponentially with chain length, the energy range that can be considered shrinks with increasing chain length. In practice, suboptimal folding can handle about a few million structures, corresponding e.g. to an energy range of say $15kT$ at a chain length of 200. An example application is shown in Fig. 2.

3 Kinetics of RNA folding

The algorithms described above provide tools to study in detail the equilibrium properties of an RNA molecule, but tell us little about the *kinetics* of the folding process. The assumptions that an RNA molecule folds into its thermodynamic ground state may well be wrong even for moderately long sequences. [26] Consequently, several groups have designed kinetic folding algorithms for RNA secondary structures, mostly in an attempt to get more accurate predictions or in in order to include pseudo-knots, see e.g. [27,28,29,30,31] Only a few work have attempted to reconstruct folding pathways. [32,33,34]

A crucial ingredient for the simulation of RNA folding is the choice of a "move set" for inter-converting secondary structures. This move-set defines the topology of the energy landscape by defining which secondary structures are neighbors of each other and encodes the set of structural changes that RNAs can undergo with moderate activation energies. The algorithms cited above generally operate on a list of all possible helices and consequently use move-sets that destroy or form entire helices in a single move. Such a move-set can introduce large structural changes in a single move and furthermore, ad hoc assumptions have to made about the rates of helix formation and disruption. A more local move-set is, therefore, preferable if one hopes to observe realistic folding trajectories.

The most elementary move-set, on the level of secondary structures, consists of removal and insertion of single base pairs (while making sure that Eq. 1 is not violated). In our simulations we use either this simple move-set or, as in the simulations shown below, base pair insertion and deletions plus base pair "flips" in which a base pair $[i, j]$ is converted into a new pair $[i, k]$. These flip moves facilitate sliding of the two strands of helix, which is assumed to be an important effect in dynamics of RNA molecules.

We simulate the dynamics by an algorithm designed for stochastic chemical reactions by Gillespie. [35] It is a variant of the Monte Carlo algorithm without rejections, in which the rate constants from the current conformation to all neighbors are computed before a new conformation and the time increment are chosen.

For the rates themselves we assume a symmetrical rule $k \sim \exp(-\Delta G/2kT)$ independent of the sign of ΔG instead of the usual Metropolis rule. For a discussion of other possibilities see e.g. [36,37] A few additional simulation were run using the Metropolis rule and showed qualitatively similar results.

To fix the time scale of our simulations we have looked at the small hairpin formed by the `AAAAAACCCCCCUUUUUU` oligonucleotide measured by Pörschke. [38]

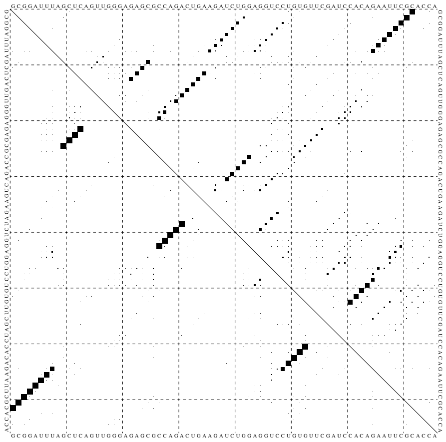

Figure 3: Base pair probabilities for an Phenylalanine tRNA with and without modified bases. The equilibrium frequency p of a pair $[i, j]$ is represented by a square of area p in position i, j and j, i of the matrix. Lower left: only base pairs contained in the ground state occur with significant frequency for the sequence with modified bases. Upper right: The unmodified sequence displays a large number of base pairs from suboptimal structures, although the ground state remains unchanged.

Since we have not yet compared our simulations with measurements on longer RNA molecules, the times given in the figures below should only be taken as rough estimates.

Folding kinetics of tRNA$^{\text{phe}}$ *and the effect of modified bases*

As a first application we shall analyze the folding kinetics of the well known phenylalanine tRNA from yeast in the remainder of this contribution.

tRNA molecules from most organisms contain several modified bases, particularly methylations. These modified bases occur mostly in unpaired regions and often the modifications are such that base pairing is made impossible. Hence, one might speculate that the modified bases help to stabilize the correct fold.

The phenylalanine tRNA from yeast used in the following contains six modification which prohibit base pairing its 76 nucleotides. As can be seen in Fig. 3 the modifications have a strong effect on the equilibrium ensemble of structures. The frequency of the correct fold in the thermodynamic ensemble rises from 4.4% to 28% and suboptimal folding shows that the lowest six suboptimal structure are prohibited by the modifications and consequently the energy gap from the ground state to next the possible structures increases from 0.4 to 0.9 kcal/mol. The density of states for the modified sequence can also be seen in Fig. 2.

Local minima are of particular importance for the folding dynamics. We have checked all configuration within 15 kcal/mol of the ground state for local optima using the same move-set as in the folding simulation. The resulting distributions can be seen in the lower part of Fig. 2. The modified sequence exhibits very few local minima in the low energy region, there are only 10 local minima within 5 kcal/mol of

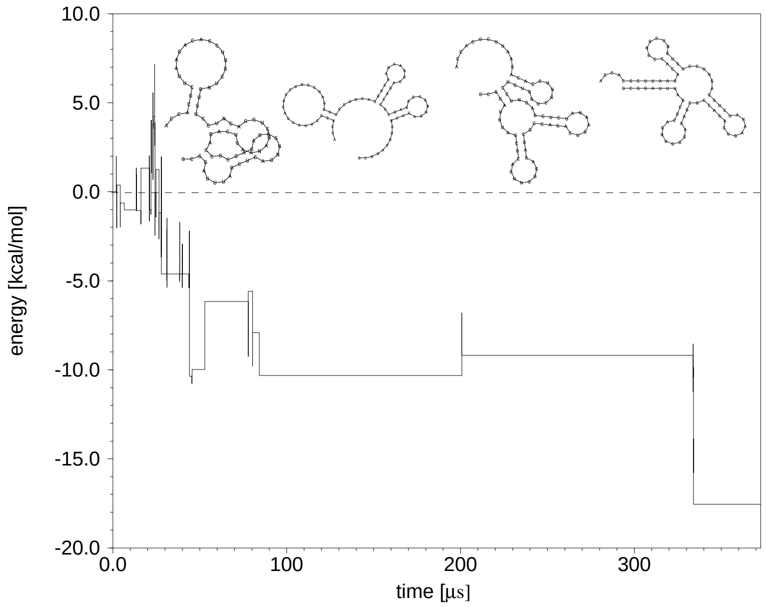

Figure 4: Energy as a function of time for a representative simulation of the modified tRNA. A few intermediate structures are shown at the top, the last one being the native cloverleaf structure. The stem closing the multi-loop forms last in most simulations.

the ground state compared to 173 for the unmodified sequence (not shown). Finding low energy local minima is an example for the analysis of the folding landscape made possible by the new suboptimal folding algorithm, without resorting to complete enumeration of structures.[39]

To study the kinetic effect of the modifications, we have simulated the folding of modified and unmodified tRNA sequence in 1000 simulations each. The resulting trajectories were then analyzed for the existence of typical folding pathways. Data from a representative simulation are shown in Fig. 4. In this particular run the RNA folds somewhat slower than average, but nevertheless shows features common to all trajectories. A rapid collapse leads to a structure with almost as many base pairs as the native state but little overlap. Folding then proceeds through a series of local minima that have more and more structural elements in common with the ground state. The waiting times in the local minima increase with decreasing energy. Many trajectories visit the same low energy intermediates, in particular, the stem closing the multi-loop forms last in almost all simulations. Interestingly, the correct hairpins closest to the 5'-end are often formed first, which might support efficient folding during transcription.

As a measure of foldability we recorded the folding times, i.e. the time after which the ground state appears in the simulation for the first time. The resulting distribution can be seen in Fig. 5. For the modified sequence the ground state was found in all simulations. This is consistent with recent analysis by Thirumalai[40] of experimental data, suggesting a directed pathway to the native state for tRNAs.

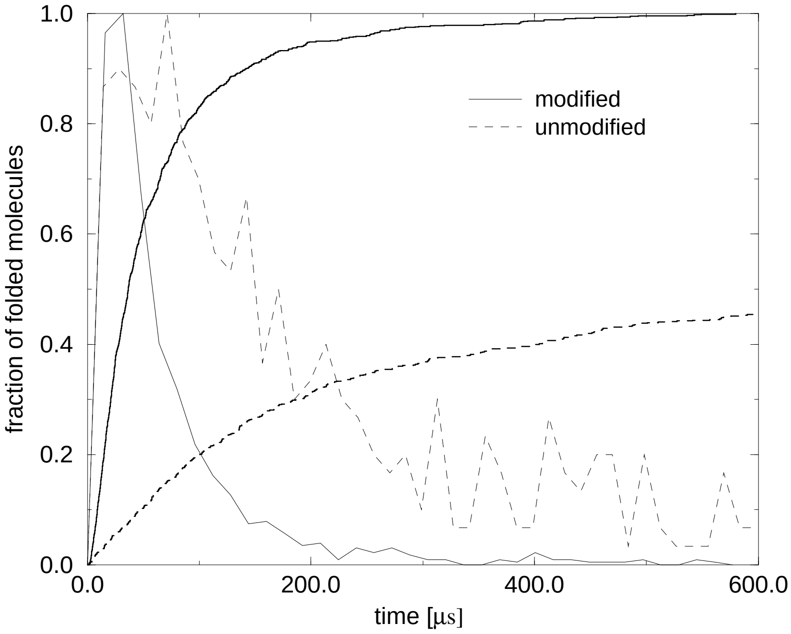

Figure 5: Folding kinetics of modified and unmodified Phenylalanine tRNA. Thick lines show the fraction of simulations that have found the ground state as a function of time. Thin lines show the distribution of folding times, scaled such that the maximum has height one. 1000 simulations were run for each sequence. While the modified sequence folds very efficiently, the unmodified sequences do not find the correct fold within the simulation time in over 50% of the cases.

The unmodified sequence folds much more slowly and only 46% of runs reach the ground state within the simulation time. The fraction of folded sequences is still rising at that point and longer simulation will be needed to decide whether the curve saturates at less than unity.

In case of the phenylalanine tRNA the modified bases improved both thermodynamic stability, conferred by a large energy gap between native and mis-folded states, and foldability. The same link has been claimed for lattice protein models by Săli et.al. [41] To test this hypothesis we have designed two artificial sequences with the tRNA structure as ground state using the `RNAinverse` program from the `Vienna RNA Package`. The thermodynamics of the first sequence are average, the frequency of the ground state in the ensemble is about 7% and several alternative foldings can be seen in the base pair probability matrix, see inset of Fig. 6. The other sequence had been designed to especially stable. For this sequence the ground state dominates the ensemble with a frequency of 96% and no alternative foldings are discernible in the dot plot. We than ran 1000 folding simulations for each sequence the results of which can be seen in Fig. 6. Surprisingly, it is the thermodynamically more stable sequence that folds poorly in this example.

Even an isolated example such as this one shows that it is easy to construct cases where the kinetics cannot be predicted from thermodynamic properties. More test cases will be needed in order to decide if and how strongly thermodynamic stability and foldability correlate on average.

Conclusion

The dynamics of RNA folding have so far received relatively little attention, especially compared to the wealth of experimental and theoretical work on protein folding dynamics. Nevertheless, RNA secondary structures provide a promising model of biopolymer folding, the main advantage being that most thermodynamic quantities of interest can be computed exactly and simulations are necessary only for truly dynamical aspects such as folding pathways. Furthermore, RNA secondary structures combine simplicity, comparable to lattice models of protein folding, with a realistic energy model that allows to study biologically relevant sequences.

Folding simulations of natural and artificial tRNA sequences exhibit cases were the sequence finds the native state efficiently and often via the same intermediate structures, as well as cases were a large fraction of runs get trapped in local minima from which they cannot escape on the time-scale of the simulation. By prohibiting base pairing for a few crucial nucleotides, the base modifications present in natural tRNAs strongly bias the folding kinetics as well as the equilibrium ensemble towards the native state.

Acknowledgments

The research on RNA folding dynamics is an on-going joint effort with Peter Schuster, Walter Fontana, and Peter Stadler at our Institute in Vienna. The folding simulations are part of the dissertation work of Christoph Flamm. The suboptimal folding algorithm was designed by Stefan Wuchty during his masters thesis.

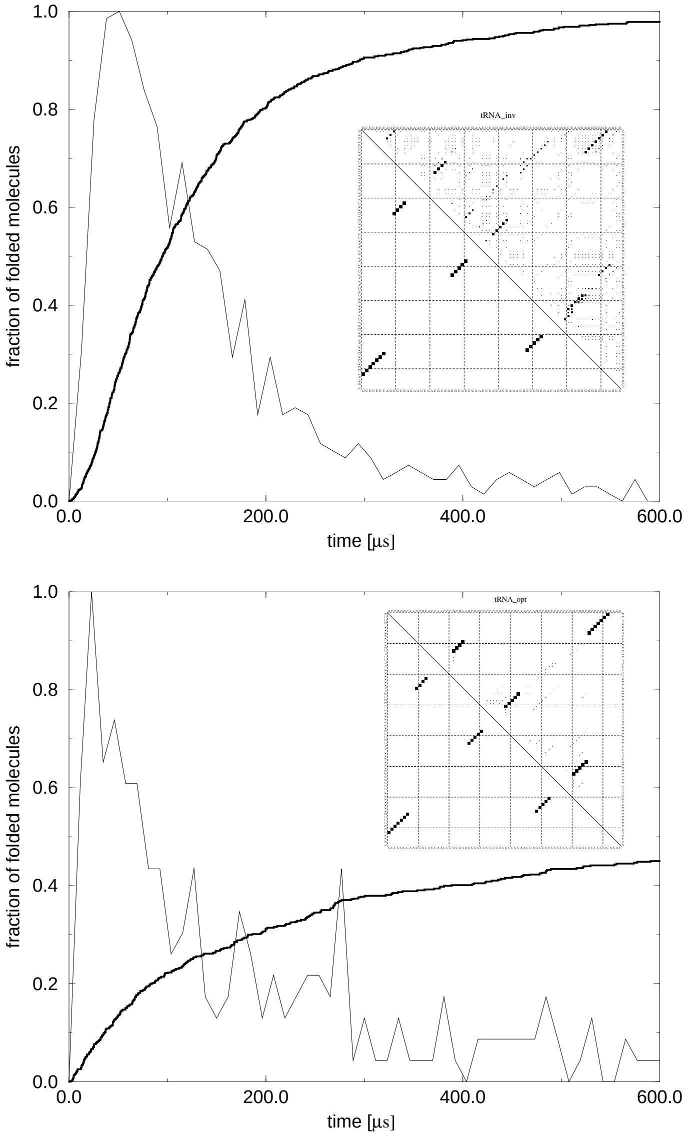

Figure 6: Thermodynamic stability and "foldability". Fraction of folded sequences as a function of time and folding times for two artificial sequences designed to fold into the tRNA cloverleaf structure. Inset: dot plots showing the equilibrium base pair probabilities (upper right) as obtained from McCaskill's algorithm and the contact map of the tRNA structure (lower left). Top: a randomly chosen sequence with tRNA structure shows many alternative foldings in the dot plot but nevertheless folds efficiently. Bottom: A sequence designed to be thermodynamically extra stable (see inset) folds only in less than 50% of the simulations.

References

1. D. E. Draper. Parallel worlds. *Nature Struct. Biol.*, 3:397–400, 1996.
2. Walter Fontana, D. A. M. Konings, P. F. Stadler, and P. Schuster. Statistics of RNA secondary structures. *Biopolymers*, 33:1389–1404, 1993.
3. Walter Fontana, Peter F. Stadler, Erich G. Bornberg-Bauer, Thomas Griesmacher, Ivo L. Hofacker, Manfred Tacker, Pedro Taranzona, Edward D. Weinberger, and Peter Schuster. RNA folding and combinatory landscapes. *Physical Review E*, 47(3):2083–2099, 1993.
4. P. Schuster, W. Fontana, P. F. Stadler, and I. L. Hofacker. From sequences to shapes and back: A case study in RNA secondary structures. *Proc. Royal Society London B*, 255:279–284, 1994.
5. Martijn A. Huynen, Peter F. Stadler, and Walter Fontana. Smoothness within ruggedness: the role of neutrality in adaptation. *Proc. Natl. Acad. Sci. (USA)*, 93:397–401, 1996.
6. Eric Westhof and Luc Jaeger. RNA pseudoknots. *Current Opinion Struct. Biol.*, 2:327–333, 1992.
7. Susan M. Freier, Ryszard Kierzek, John A. Jaeger, Naoki Sugimoto, Marvin H. Caruthers, Thomas Neilson, and Douglas H. Turner. Improved free-energy parameters for prediction of RNA duplex stability. *Proc.Natl.Acad.Sci.USA*, 83:9373–9377, 1986.
8. J. A. Jaeger, D. H. Turner, and M. Zuker. Improved predictions of secondary structures for RNA. *Proc. Natl. Acad. Sci. USA*, 86:7706–7710, 1989.
9. Amy E. Walter, Douglas H. Turner, James Kim, Matthew H. Lyttle, Peter Müller, David H. Mathews, and Michael Zuker. Co-axial stacking of helixes enhances binding of oligoribonucleotides and improves predicions of rna folding. *Proc. Natl. Acad. Sci. USA*, 91:9218–9222, 1994.
10. M. S. Waterman. Secondary structure of single - stranded nucleic acids. *Studies on foundations and combinatorics, Advances in mathematics supplementary studies, Academic Press N.Y.*, 1:167 – 212, 1978.
11. M. S. Waterman and T. F. Smith. RNA secondary structure: A complete mathematical analysis. *Mathematical Biosciences*, 42:257–266, 1978.
12. Ruth Nussinov, George Piecznik, Jerrold R. Griggs, and Daniel J. Kleitman. Algorithms for loop matching. *SIAM J. Appl. Math.*, 35(1):68–82, 1978.
13. Ruth Nussinov and Ann B. Jacobson. Fast algorithm for predicting the secondary structure of single-stranded RNA. *Proc. Natl. Acad. Sci. USA*, 77(11):6309–6313, 1980.
14. M. Zuker and P. Stiegler. Optimal computer folding of larger RNA sequences using thermodynamics and auxiliary information. *Nucleic Acids Research*, 9:133–148, 1981.
15. M. Zuker and D. Sankoff. RNA secondary structures and their prediction. *Bull.Math.Biol.*, 46(4):591–621, 1984.
16. M. Zuker. On finding all suboptimal foldings of an RNA molecule. *Science*, 244:48–52, 1989.
17. John S. McCaskill. The equilibrium partition function and base pair binding probabilities for RNA secondary structure. *Biopolymers*, 29:1105–1119, 1990.

18. Ivo L. Hofacker, Martijn A. Huynen, Peter F. Stadler, and Paul E. Stolorz. Knowledge discovery in rna sequence families of HIV using scalable computers. In Evangelos Simoudis, Jiawei Han, and Usama Fayyad, editors, *Proceedings of the 2nd International Conference on Knowledge Discovery and Data Mining, Portland, OR*, pages 20–25, Menlo Park, CA, 1996. AAAI Press.
19. Martijn A. Huynen, Alan S. Perelson, Wayne A. Vieira, and Peter F. Stadler. Base pairing probabilities in a complete HIV-1 RNA. *J. Comp. Biol.*, 3:253–274, 1996. SFI preprint 95-07-057, LAUR-95-1613.
20. I. L. Hofacker, W. Fontana, P. F. Stadler, and P. Schuster. `Vienna RNA Package`. `http://www.tbi.univie.ac.at/ ivo/RNA/`, 1994. (Free Software).
21. Ivo L. Hofacker, Walter Fontana, Peter F. Stadler, Sebastian Bonhoeffer, Manfred Tacker, and Peter Schuster. Fast folding and comparison of RNA secondary structures. *Monatsh. Chem.*, 125(2):167–188, 1994.
22. Jan Cupal, Ivo L. Hofacker, and Peter F. Stadler. Dynamic programming algorithm for the density of states of RNA secondary structures. In R. Hofstädt, T. Lengauer, M. Löffler, and D. Schomburg, editors, *Computer Science and Biology 96 (Proceedings of the German Conference on Bioinformatics)*, pages 184–186, Leipzig (Germany), 1996. Univeristät Leipzig.
23. Jan Cupal. The density of states of rna secondary structures. Master's thesis, University of Vienna, 1997.
24. P. G. Higgs. RNA secondary structure: a comparison of real and random sequences. *J.Phys.I (France)*, 3:43, 1993.
25. Stefan Wuchty. Suboptimal secondary structures of rna. Master's thesis, Univiersity of Vienna, 1998.
26. S. R. Morgan and P. G. Higgs. Evidence for kinetic effects in the folding of large RNA molecules. *J. Chem. Phys.*, 105:7152–7157, 1996.
27. H. M. Martinez. An RNA folding rule. *Nucl.Acid.Res.*, 12:323–335, 1984.
28. A. A. Mironov, L. P. Dyakonova, and A. E. Kister. A kinetic approach to the prediction of RNA secondary structures. *J. Biomol. Struct. Dynam.*, 2(5):953 – 962, 1985.
29. J. P. Abrahams, M. van den Berg, E. van Batenburg, and C. Pleij. Prediction of RNA secondary structure, including pseudoknotting, by computer simulation. *Nucl. Acids Res.*, 18:3035–3044, 1990.
30. A. P. Gultyaev. The computer simulation of RNA folding involving pseudoknot formation. *Nucl. Acids Res.*, 19:2489–2493, 1991.
31. Manfred Tacker, Walter Fontana, Peter F. Stadler, and Peter Schuster. Statistics of RNA melting kinetics. *Eur. Biophys. J.*, 23:29–38, 1994.
32. P. G. Higgs. Thermodynamic properties of transfer RNA: A computational study. *J.Chem.Soc.Faraday Trans.*, 91(16):2531–2540, 1995.
33. A.P. Gultyaev, Van Batenburg, and CWA Pleij. The computer simulation of rna folding pathways using an genetic algorithm. *J.Mol.Biol.*, 250:37–51, 1995.
34. A.A. Suvernev and P.A. Frantsuzov. Statistical description of nucleic acid secondary structure folding. *J. Biomolec. Struct. Dyn.*, 13:135–144, 1995.
35. D. T. Gillespie. *J. Comput. Phys.*, 22:403, 1976.

36. P. G. Higgs and S R Morgan. Thermodynamics of rna folding. when is an RNA molecule in equilibrium. In F. Morán, A. Moreno, J.J. Merelo, and Chacón, editors, *Advances in Artificial Life*, pages 852–861, Berlin, 1995. ECAL 95, Springer Verlag.
37. Hue Sun Chan and Ken A. Dill. Protein folding in the landscape perspective: Chevron plots and non-Arrhenius kinetics. *Proteins: Structure, Function, and Genetics*, 30:2–33, 1998.
38. D. Pörschke. Thermodynamic and kinetic parameters of an oligonucleotide hairpin helix. *Biopys. Chem.*, 1:381–386, 1974.
39. Jan Cupal, Christoph Flamm, Alexander Renner, and Peter F. Stadler. Density of states, metastable states, and saddle points. Exploring the energy landscape of an RNA molecule. In T. Gaasterland, P. Karp, K. Karplus, Ch. Ouzounis, Ch. Sander, and A. Valencia, editors, *Proceedings of the ISMB-97*, pages 88–91, Menlo Park, CA, 1997. AAAI Press.
40. D. Thirumalai and S.A. Woodson. Kinetics of folding of proteins and RNA. *Acc. Chem. Res.*, 29:433–439, 1996.
41. A. Šali, E. Shakhnovich, and M. Karplus. Kinetics of protein folding. A lattice model study on the requirements for folding of native states. *J. Mol. Biol.*, 253:1614–1636, 1994.